BIOCHEMISTRY
including biophysical chemistry & molecular biology
Article

Biochemistry **2011,** *50,* 17–24 17
DOI: 10.1021/bi1013112

A Combined Fluorescence Spectroscopic and Electrochemical Approach for the Study of Thioredoxins[†]

Mariana Voicescu,[‡,||] Dagmar Rother,[§] Frank Bardischewsky,[§] Cornelius G. Friedrich,[§] and Petra Hellwig*[,‡]

[‡]*Laboratoire de Spectroscopie Vibrationnelle et Electrochimie des Biomolécules, UMR 7177, Institut de Chimie, CNRS-Université de Strasbourg, 1 rue Blaise Pascal, 67070 Strasbourg, France, and* [§]*Lehrstuhl für Technische Mikrobiologie, Fachbereich Bio- und Chemieingenieurwesen, Technische Universität Dortmund, Emil-Figge-Strasse 66, 44221 Dortmund, Germany.*
[||]*Permanent address: Romanian Academy, Institute of Physical Chemistry "Ilie Murgulescu", Splaiul Independentei 202, 060021 Bucharest, Romania.*

Received August 16, 2010; Revised Manuscript Received November 24, 2010

ABSTRACT: A new way to study the electrochemical properties of proteins by coupling front-face fluorescence spectroscopy with an optically transparent thin-layer electrochemical cell is presented. First, the approach was examined on the basis of the redox-dependent conformational changes in tryptophans in cytochrome *c*, and its redox potential was successfully determined. Second, an electrochemically induced fluorescence analysis of periplasmic thiol-disulfide oxidoreductases SoxS and SoxW was performed. SoxS is essential for maintaining chemotrophic sulfur oxidation of *Paracoccus pantotrophus* active in vivo, while SoxW is not essential. According to the potentiometric redox titration of tryptophan fluorescence, the midpoint potential of SoxS was -342 ± 8 mV versus the standard hydrogen electrode (SHE′) and that of SoxW was -256 ± 10 mV versus the SHE′. The fluorescence properties of the thioredoxins are presented and discussed together with the intrinsic fluorescence contribution of the tyrosines.

Periplasmic thiol-disulfide oxidoreductases SoxS and SoxW are both formed upon oxidation of reduced sulfur compounds (Sox) of the facultative chemotrophic bacterium *Paracoccus pantotrophus*. While SoxS is an essential component for inorganic sulfur oxidation of *P. pantotrophus* in vivo, it was reported that SoxW is not required (*1*−*3*). These proteins are members of the thioredoxin superfamily that are typically distinguished by their redox partners and functions in the dithiol/disulfide structure of proteins. They carry a Cys-Xaa-Xaa-Cys active-site sequence motif and are able to reduce protein disulfides. SoxS specifically reduces an interprotein disulfide that renders a key protein of the system inactive (*4*, *5*). In this work, we aim to analyze the redox potential of the thioredoxin-like proteins from *P. pantotrophus*.

Redox electrochemistry of proteins relying on classical techniques like cyclovoltamperometry is often hindered by the unspecific absorption to the electrodes (*6*−*8*). For several proteins, the redox-dependent change of a signal in the visible spectral range was successfully used to characterize the proteins in solution. However, because the thioredoxin-like proteins do not absorb in the visible spectral range, a different solution was required. Fluorescence techniques rely on tyrosine (Tyr), phenylalanine (Phe), and tryptophan (Trp) that are the natural chromophores in proteins. Trp is the most extensively used amino acid for fluorescence analysis of proteins. In a protein containing all three fluorescent amino acids (Tyr, Trp, and Phe), the observation of Tyr and Phe fluorescence is often complicated because of the overlap by the Trp resonance energy transfer (*9*, *10*). The use of Tyr and Phe fluorescence is often limited to Trp-free protein, with few exceptions (*11*). The presence of Trp residues as intrinsic fluorophores in most proteins makes them an obvious choice for fluorescence spectroscopic analysis. Intrinsic fluorescence of proteins has been used in numerous biochemical and biophysical studies to probe protein structure and dynamics. The spectral signatures are typically influenced by the characteristics of the microenvironment and the location of the fluorophores in the protein (*12*, *13*).

The intrinsic fluorophores as well as the biochemical data of SoxS and SoxW and their His_6-tagged derivatives are listed in Table 1. They are evidently suitable for a fluorescence spectroscopic approach. We note that for both the His_6-SoxS and His_6-SoxW proteins, the MRGSHHHHHHG**SDDDDK** sequence for the enterokinase cleavage site has been added (bold).

In this study, we describe a new way to determine the midpoint potential of the proteins, by coupling front-face fluorescence spectroscopy (FFFS)[1] with an optically transparent thin-layer electrochemical (OTTLE) cell. The right-angle fluorescence spectroscopic techniques cannot be applied to solid substances or nontranslucent solutions, because of the large absorbance and scattering of light (*14*). However, Parker (*15*) developed a technique for reducing the scattering effect by changing the angle of incidence on the sample from 90° to 56°. This technique is known as front-face fluorescence spectroscopy, and it is reported that it is able to provide information at the molecular level for gels and for other dairy products, including milk and yogurt (*16*).

Previous studies based on in situ fluorescence spectroelectrochemistry are available (*17*−*21*), some of them using an optically

[†]Financial support was provided by the ANR chair, d'excellence, the Université de Strasbourg. M.V. is grateful for financial support from the CNRS.

*To whom correspondence should be addressed. E-mail: hellwig@unistra.fr. Telephone: 0033 368 851273. Fax: 0033 368 851431.

[1]Abbreviations: Cyt *c*, cytochrome *c*; FFFS, front-face fluorescence spectroscopy; OTTLE, optically transparent thin-layer electrochemical; SHE′, standard hydrogen electrode (pH 7).

Published on Web 11/29/2010

Table 1

	SoxS	SoxW	His_6-SoxS	His_6-SoxW
no. of amino acids minus leader peptide	99	166	116	183
no. of Trp residues	2	3	2	3
no. of Tyr residues	3	3	2	3
MW minus leader peptide	11077.1	18720.3	13064.76	20707.3
pI	4.29	4.78	5.05	5.11

transparent thin-layer electrode (*22*, *23*). Dias et al. (*24*) reported the efficiency of a spectroelectrochemical cell by coupling electrochemistry with fluorescence spectroscopy. Recently, a study on the combined fluorescence and electrochemical investigation of the binding interaction between organic acids and human serum albumin has been performed (*25*).

Here we have employed electrochemistry coupled to the steady-state front-face fluorescence spectroscopy to study the thioredoxin-like proteins from *P. pantotrophus*. The analysis was performed with the help of the redox-dependent change in tryptophan fluorescence. In addition, cytochrome *c* was used as a well-known probe to show that the technique leads to reliable results (*26*).

MATERIALS AND METHODS

Materials. Cytochrome *c* from horse heart (97% pure based on 6% H_2O content) was purchased from Sigma. The concentration of the cytochrome *c* was 2 mM in 45 mM Tris-HCl (pH 7.4), and all measurements were performed at 5 °C.

Thioredoxins SoxS and SoxW from *P. pantotropus* were produced as His_6-tagged proteins without leader peptides in *Escherichia coli* and purified by Ni affinity chromatography as described for SoxS (*4*).

To amplify the *soxW* gene without the signal peptide coding region, we used polymerase chain reaction (PCR). Primers S58 (5′-AAAAGGATCCGATGACGATGACAAAGCCGAAATCGGCGACGACGG-3′) and S59 (5′-TTTTAAGCTTCAGCCGAAGATGTCGGCGGTG-3′) introduced the template for an enterokinase cleavage site upstream of *soxW*. This fragment was cloned into the *Bam*HI and *Hin*dIII sites of expression vector pQE30 (Qiagen). The hexahistidine tag-coding region was specified by the vector. The resulting plasmid pRD191.10 was transformed in *E. coli* M15 also containing plasmid pREP4 (Qiagen), which delivered additional *lac* repressor.

To produce His_6-SoxW, cells were cultured aerobically at 30 °C in 1 L of LB medium supplemented with Amp^{100} and Km^{25} at 30 °C. When the OD_{600} reached 0.8, cells were induced with 0.2 mM IPTG for 4 h at 30 °C. Cells were harvested and washed twice with 50 mM potassium sodium phosphate buffer (pH 7.2) with 300 mM NaCl, 10 mM imidazole, 1 mM $MgCl_2$, and 1 mM phenylmethanesulfonyl fluoride. Cells were resuspended in the same buffer and passed three times through a French press at 8000 psi. Whole cells and cell debris were separated from soluble proteins by centrifugation at 20000 rpm and 4 °C for 30 min. The supernatant (1.1 mL with 40 mg of protein) was applied on a 6 mL Ni(II)-NTA-agarose column (Qiagen) equilibrated with resuspension buffer. The column was washed with resuspension buffer and then with the buffer containing 20 mM imidazole. His_6-SoxW was eluted with resuspension buffer containing 250 mM imidazole. His_6-SoxW-containing fractions were pooled and dialyzed against 50 mM Tris-HCl (pH 7.5) with 1 mM ethylenediaminetetraacetic acid.

The solutions were prepared in 45 mM Tris-HCl buffer (pH 7.4). Tris(hydroxymethyl)aminomethane was purchased from Sigma-Aldrich. The pH was measured using a Microprocessor pH-Meter (model pH 211) from HANNA Instruments. Ludox, AS-40 Colloidal Silica, a 40 wt % suspension in water, was purchased from Sigma-Aldrich.

Steady-State Fluorescence. The fluorescence emission spectra were recorded with a Fluorolog FL3-22 instrument equipped with a 450 W xenon lamp and a TBX 04 detector (Horiba Jobin Yvon), using 5 nm bandpasses for the excitation and emission monochromators, an increment of 1 nm for the emission monochromator, and integration times of 0.1 s. The emission spectra were corrected for the lamp, the monochromators, and the detector response. The excitation wavelengths were 275 nm (for the contribution of Tyr and Trp) and 300 nm (for the contribution of Trp). The contribution of Tyr to the total protein fluorescence is estimated by subtraction of the Trp emission spectrum (λ_{ex} = 300 nm) from that obtained at 275 nm (λ_{ex}), after normalization of the two spectra above 380 nm, where the Tyr emission is negligible.

The protein concentration after purification was 4.89 μM in 45 mM Tris-HCl (pH 7.4), and all measurements were taken at 5 °C. A dithiothreitol (DTT) solution was prepared in 45 mM Tris-HCl buffer (pH 7.4) and used within a few hours of preparation. The SoxS and SoxW proteins were incubated for 15 min in the presence of 1 mM DTT.

Time-Resolved Fluorescence. The fluorescence decay for the SoxS and SoxW protein was collected by the time-correlated single-photon counting (TCSPC) technique. The excitation source was an electroluminescent diode (NanoLED-295, Horiba Jobin Yvon) emitting at 295 nm with a bandwidth of ~12 nm giving pulses of ~730 ps for the full width at half-maximum. The NanoLED diode operated with a 1 MHz repetition rate, a coaxial delay of 70 ns, a time-to-amplitude converter (TAC) range of 50 ns, and a 14.5 nm band-pass. The decay curves were stored in 2048 channels of 0.028 ns/channel. The NanoLED pulse was recorded using a diluted Ludox solution (0.01%).

To determine the fluorescence lifetime of the SoxS and SoxW proteins, we fitted the fluorescence decay data to a triple-exponential function:

$$F(t) = \alpha_1 \exp(-t/\tau_1) + \alpha_2 \exp(-t/\tau_2) + \alpha_3 \exp(-t/\tau_3)$$

using Decay Analysis Software with reconvolution (DAS6), from Horiba Jovin Yvon.

The data were fitted using nonlinear least-squares methods (*27*). The quality of the data fit was judged using statistical parameters and graphical tests. The reduced χ^2 values were close to 1. The weighed residuals were low and uniformly distributed around zero.

Electrochemistry Coupled to the Steady-State Front-Face Fluorescence Spectroscopy. The spectroelectrochemical cell used in the steady-state front-face fluorescence analysis was

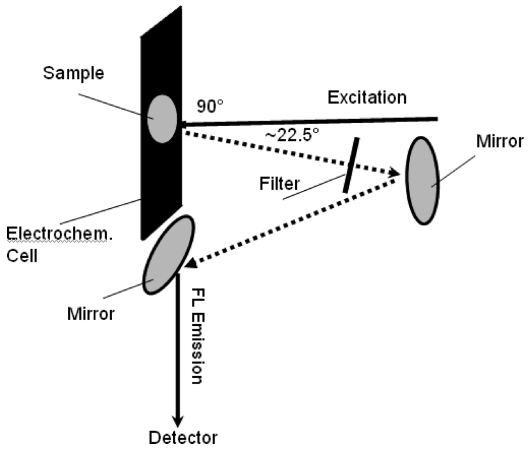

FIGURE 1: Optical pathway of electrochemically induced fluorescence analysis (adapted from Horiba Jobin Yvon Inc.).

adapted from that of Moss et al. (*28*). While the main body of the cell and the electrode geometry remained identical, the cell dimensions and the cell holder were adapted to the spectrofluorimeter.

To avoid the fluorescence contribution of the window material and to reduce the reflection, quartz windows on a support of black Plexiglas were used. A gold grid was used as the working electrode. This electrode was chemically modified with 2 mM cysteamine for 1 h and then washed with distilled water (*29*). The counter and reference electrodes were a Pt wire and an Ag/AgCl-saturated 3 M KCl electrode, respectively. The working electrode was then set into the cell and pushed against the window to form a thin layer of solution (~10 μm). For SoxS and SoxW proteins, the potential step applied was in the range of −650 to −375 mV (vs the Ag/AgCl-saturated 3 M KCl electrode); add 208 mV for the standard hydrogen electrode (SHE′) potentials.

For all electrochemical and spectroscopic experiments, samples were concentrated to the millimolar range, from 1.5 to 1.6 mM, in 45 mM Tris-HCl buffer (pH 7.4); KCl was added to a final concentration of 100 mM. The working protein solution volume was ~7 μL. To accelerate the redox reactions, we added a mixture of 18 mediators at substoichiometric concentrations of 40 μM each to the protein solution (*29*). The midpoint potentials for each used mediator are given in parentheses: ferrocenyltrimethylammonium iodide (643 mV), 1,1′-dicarboxylferrocene (642 mV), diethyl-3-methylparaphenylenediamine (365 mV), ferricyanide (422 mV), dimethylparaphenylenediamine (369 mV), 1,1′-dimethylferrocene (339 mV), tetramethylparaphenylenediamine (268 mV), tetrachlorobenzoquinone (278 mV), 2,6-dichlorophenolindophenol (215 mV), ruthenium hexamine chloride (198 mV), 1,2-naphthoquinone (−143 mV), trimethylhydroquinone (98 mV), menadione (−14 mV), 2-hydroxy-1,4-naphthoquinone (−127 mV), anthraquinone 2-sulfonate (−227 mV), neutral red (−309 mV), benzyl viologen (−362 mV), and methyl viologen (−448 mV) (*29*). The absence of a noticeable fluorescence contribution from the mediators was verified in control experiments with the buffer and the mediators alone.

The cover lid of the cell holder of the spectrofluorimeter was also adapted to have a connection among the spectroelectrochemical cell, the potentiostat (for electrochemical monitoring and recording), and a water thermostat; the cell was kept at 5 °C. The optical pathway for the coupling of the front-face fluorescence spectroscopy device with the spectroelectrochemical cell was adapted from Horiba Jobin Yvon Inc. and is presented in Figure 1. One difficulty in taking OTTLE measurements was the fact that quantitative kinetic information is based on the large electrode area whereas the solution volume is very small. This feature is more readily retrieved using specular reflectance spectroscopy, where the light passes through the solution twice upon reflection on the electrode (*30*). A greater sensitivity could be obtained by using a grazing incidence.

The spectroelectrochemical cell, inserted into a support, was mounted in the central interior of the cell holder of the spectrofluorimeter on a plate support. To obtain the best fluorescence and electrochemical responses, the angle between the spectroelectrochemical cell and the plate support was 90°. Moreover, the support of the cell was constructed in a way that it permitted the fine adjustment of the angular position in relation to the excitation beam. As one can see in Figure 1, the excitation beam from a 450 W xenon lamp was emitted at an angle of 90° relative to the surface of the working electrode, then reflected through the first mirror, and launched on the second mirror, which is found between the cell holder and detector. Here the emission fluorescence signal was collected. The incidence angle of the excitation radiation was set at 22.5° to ensure that the reflected light and scattered radiation phenomena were minimized. Essentially, the front-face illumination geometry leads the excitation and emission beam in such a way that the fluorescence emission is finally collected by the detector at a right angle. Moreover, the relation between the transmission of the optics and the detector response is wavelength-dependent.

For the excitation 10 nm bandpass and for the emission 5 nm bandpass monochromators, an increment of 1 nm for the emission monochromator and an integration time of 1 s were used. The emission spectra were corrected for the lamp, the monochromator, and the detector response. The excitation wavelengths were 275, 280, 295, and 300 nm.

Via application of a potential to the working electrode, the electron transfer process induced a normal quenching of the Trp fluorescence. The Trp fluorescence intensity, with an emission wavelength between 320 and 345 nm, was then monitored and recorded.

RESULTS AND DISCUSSION

Steady-State Fluorescence Analysis of SoxS and SoxW. The fluorescence emission spectra of SoxS were recorded at two excitation wavelengths, 275 and 300 nm. The fluorescence emission maximum was almost the same for both excitation wavelengths. Fluorescence emission was observed at 337−340 nm (λ_{em}), a fluorescence typical for tryptophans localized in a hydrophobic environment (Figure 2A). SoxS belongs to the thioredoxin 1 family founded with *E. coli* thioredoxin 1 with an active site that comprises residues Gly-^{13}Cys-Leu-Tyr-^{16}Cys-Ala (the numbering is based on the periplasmic form of the SoxS protein without the periplasmic leader peptide) (*4*). It was found that SoxS exhibits a kink within α-helix α1, which contains the active site at its N-terminal end, caused by a conserved ^{25}Pro residue that is common for other thioredoxins. This behavior implies that the active site becomes more accessible to the environment (*4*). On the basis of the sequence alignment with the known members of the thioredoxin family (*31*, *32*), the ^{19}Trp residue can be found in the proximity of the ^{15}Tyr residue, from the active site, ^{13}Cys-Leu-Tyr-^{16}Cys. They can be expected to contribute at least partially to the spectrum seen here.

The fluorescence emission spectra of SoxW at 320−323 nm (λ_{em}) (Figure 2B) probably involve a Tyr contribution. In direct

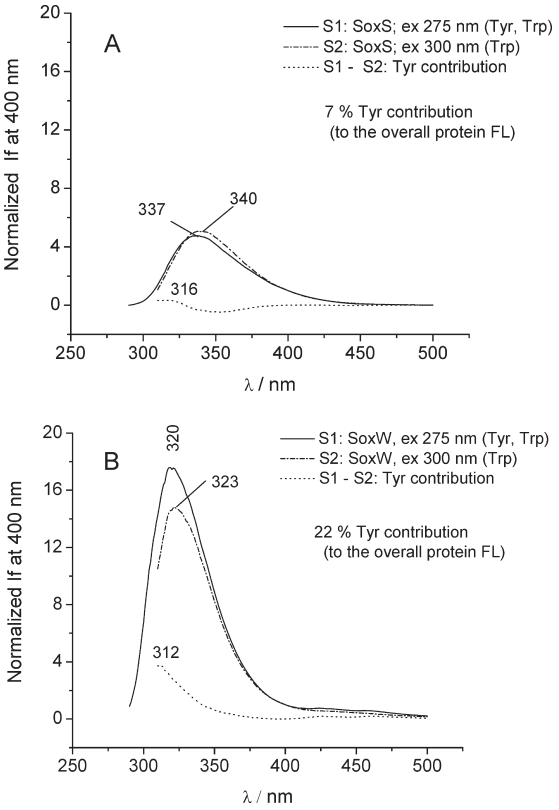

FIGURE 2: Fluorescence emission spectra of the SoxS (A) and SoxW (B) proteins. Spectra S_1 and S_2 were obtained with 275 and 300 nm excitation, respectively. The Tyr contribution was calculated as a difference between spectra S_1 and S_2 after their normalization at 400 nm. The protein concentration was 4.89 μM in 45 mM Tris-HCl (pH 7.4), and the experiments were conducted at 5 °C.

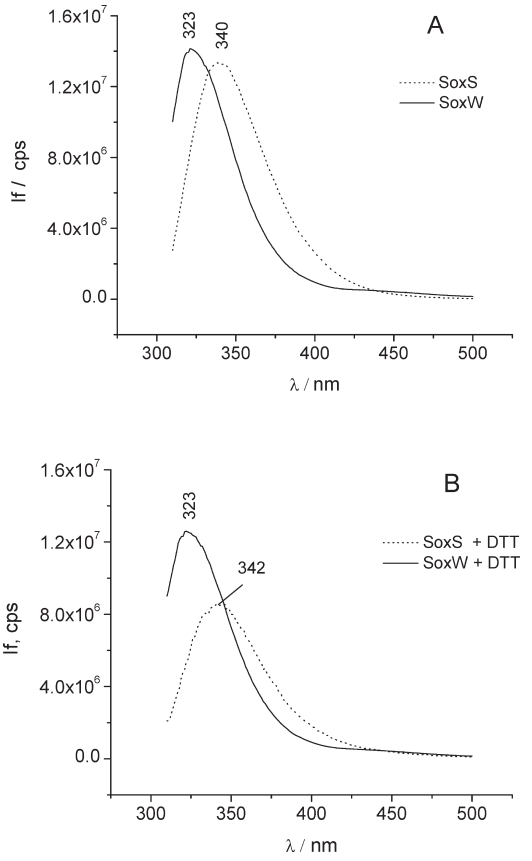

FIGURE 3: Fluorescence emission spectra of the SoxS and SoxW proteins (A) and their reaction due to the presence of DTT (B). The protein concentration was 4.89 μM in 45 mM Tris-HCl (pH 7.4), and the DTT concentration was 1 mM. The experiments were conducted at 5 °C; λ_{ex} = 300 nm.

comparison to SoxS (λ_{em} = 340 nm), the blue-shifted Trp emission (323 nm) reflected the existence of a buried Trp residue. The contribution of Tyr fluorescence to the overall protein emission was calculated (see Materials and Methods) and represented ~7% for SoxS (the Tyr fluorescence emission has a maximum at 316 nm) and 22% for SoxW; here the Tyr fluorescence emission has a maximum at 312 nm (Figure 2A). Overall, the fluorescence emission spectra of the SoxS and SoxW proteins showed a fluorescence emission that is essentially caused by the Trp residues and a minor contribution caused by Tyr residues.

To fully reduce the disulfide bonds of the thioredoxins, we recorded fluorescence emission spectra of SoxS and SoxW in the presence of DTT. In the case of SoxS, reduction of the disulfide bond caused a 1.5-fold decrease in fluorescence intensity and a 2 nm red shift (Figure 3A). This behavior was mainly due to a Trp residue. For the SoxW protein, no shift in the wavelength of the emission maximum was observed and the fluorescence intensity was slightly decreased (Figure 3B). These results implied that the changes induced upon reduction were small for this protein. SoxW does not have a Trp close to the active-site helix; although ^{20}Asp is close to ^{16}Cys, ^{19}Trp seems to stick out. An exposure of ^{19}Trp to a lower surface hydrophobicity upon reduction of the disulfide bonds may be considered.

Time-Resolved Fluorescence Analysis of SoxS and SoxW. Fluorescence lifetime measurements have been previously used to study the existence of different and unique conformations (*33*). Conventionally, the decay is resolved in terms of exponential components, and the values of the decay rates and pre-exponential factors of each component are associated with a particular conformation and with the relative population of each conformation (*33*, *34*). The fluorescence decay kinetics of the SoxS and SoxW proteins were studied in the nanosecond domain and fitted to the linear combination of triple exponentials (Figure 4). The fluorescence decay parameters of SoxS and SoxW are summarized in Table 2. Three components with different rates of decay indicating different conformers were found. The location of the Trp residues related to the secondary structure was taken into consideration. The long fluorescence lifetime (τ_2) corresponded to the local changes in the configuration between Trp and the S−S bond. The medium and short fluorescence lifetimes (τ_1 and τ_3, respectively) were attributed to the electron transfer process from excited Trp to the peptide bond. The SoxS and SoxW thioredoxin motifs, CLYC and CIYC, respectively, are distinct with respect to the inner amino acids from those of other thioredoxins (*35*). Therefore, the results were associated with the local environment of SoxW and SoxS Trp residues and subsequently with the environment of the S−S bond at the active site.

Electrochemically Induced Steady-State Front-Face Fluorescence Analysis. (*i*) *Electrochemical Behavior Tested for Cytochrome c*. Cytochrome *c* from horse heart contains a Trp and four Tyr residues (*36*). The steady-state front-face fluorescence emission spectra were recorded using a solution of 2 mM Cyt *c* in 0.1 M phosphate buffer (pH 8) at 5 °C for two excitation wavelengths, 275 and 280 nm. The fluorescence emission appears at 321 nm, specific for a buried Trp residue

Table 2: Fluorescence Decay Parameters of the SoxS and SoxW Proteins[a]

protein	τ_1 (ns) (%)	τ_2 (ns) (%)	τ_3 (ns) (%)	χ_R^{2b}
SoxS (9.78 μM)	2.04 (9) ± 0.0000943[c]	7.32 (86) ± 0.0000300	0.18 (5) ± 0.0004294	1.02
SoxW (6 μM)	1.36 (20) ± 0.0001529	3.89 (69) ± 0.0000400	0.33 (11) ± 0.000332	1.21

[a]The proteins were in 45 mM Tris-HCl (pH 7.4), and the experiments were conducted at 5°C. λ_{ex} = 295 nm, and the relative contribution of each component is given in parentheses. [b]χ_R^2 is the quality of the fit, and the residual goodness of fit values were determined for three-component fits. [c]The uncertainties in the lifetimes and in the percentage of amplitudes were obtained by exponential analysis of the fluorescence decay.

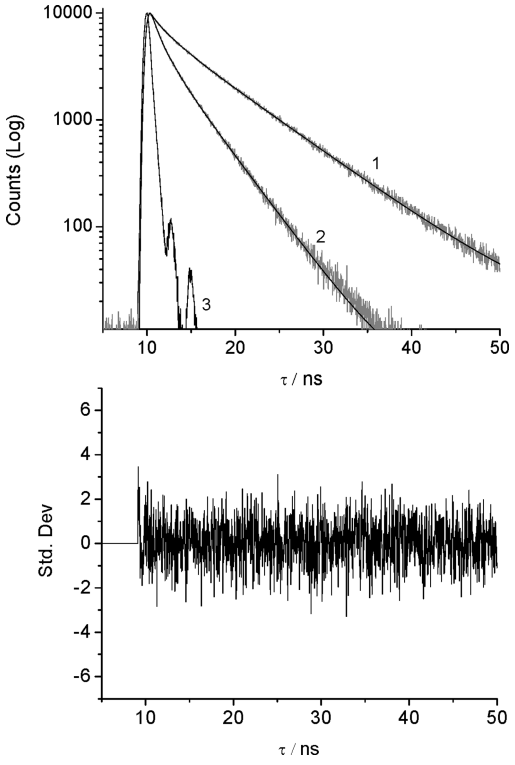

FIGURE 4: Fluorescence decay curves of SoxS (1) and SoxW (2) in 45 mM Tris-HCl (pH 7.4). NanoLED pulse (3) (λ_{ex} = 295 nm) and random distribution of weighted residuals (λ_{em} = 320 nm). Resolution of 0.028 ns/channel.

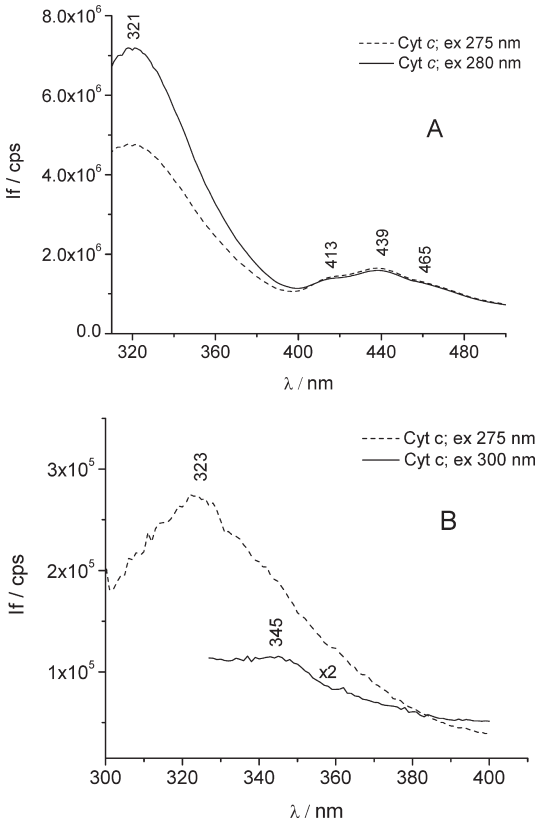

FIGURE 5: Steady-state front-face fluorescence emission spectrum of Cyt *c* from horse heart, without an applied potential. (A) The measurements were recorded at 5 °C for 2 mM Cyt *c* in 0.1 M phosphate buffer (pH 8). (B) The measurements were performed at room temperature for a 2 mM aqueous solution of Cyt *c*.

(Figure 5A). For the aqueous solution of Cyt *c* and using excitation wavelengths of 275 nm at 5 °C and 300 nm at room temperature, the fluorescence emission spectra have maxima at 323 and 345 nm, respectively (Figure 5B). Using an excitation wavelength of 300 nm, a slight decrease in fluorescence intensity with a 4 nm red shift (from 342 to 348 nm) was found when the applied potential becomes oxidative. Two isosbestic points were observed at 353 and 417 nm (Figure 6). For the control, the same experiment was repeated for an excitation wavelength of 280 nm, and potential steps from −250 and 150 mV have been used (data not shown). Here the steady-state front-face fluorescence emission was observed at 321 nm and a gradual decrease in fluorescence intensity also evidenced. The isosbestic point was found at 340 nm.

Cyt *c* was potentiometrically titrated on the basis of its fluorescence intensity at 321 nm, when the potential applied to the working electrode is in the range from −150 to 150 mV (Figure 7). The data as analyzed with a theoretical Nernst fit determined the number of transferred electrons to be one. The Nernst fit of the fluorescence titration resulted in a midpoint potential of 22 ± 10 mV versus Ag/AgCl. The reductive titration revealed a redox potential of 48 ± 20 mV versus Ag/AgCl (data not shown). These values are in agreement with the midpoint

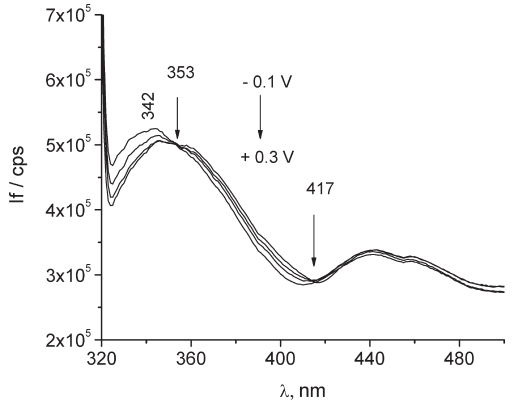

FIGURE 6: Steady-state front-face fluorescence emission spectrum of Cyt *c* from horse heart. The Cyt *c* concentration was 2 mM in 0.1 M phosphate buffer (pH 8). The measurements were taken at 5 °C in a potential range applied from −100 to 300 mV. The excitation wavelength was 300 nm.

potential of Cyt *c* in solution, around 50 mV, reported in the literature (*37*).

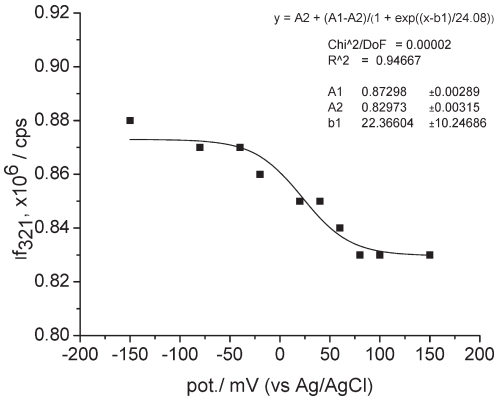

FIGURE 7: Potentiometric titration of Cyt *c* from horse heart. The Nernst fit of the fluorescence intensity at 321 nm led to a midpoint potential of 22 ± 10 mV vs Ag/AgCl. The Cyt *c* concentration was 2 mM in 45 mM Tris-HCl (pH 7.4), and the measurements were taken at 5 °C. The excitation wavelength was 280 nm. The potential range applied was from −150 to 150 mV.

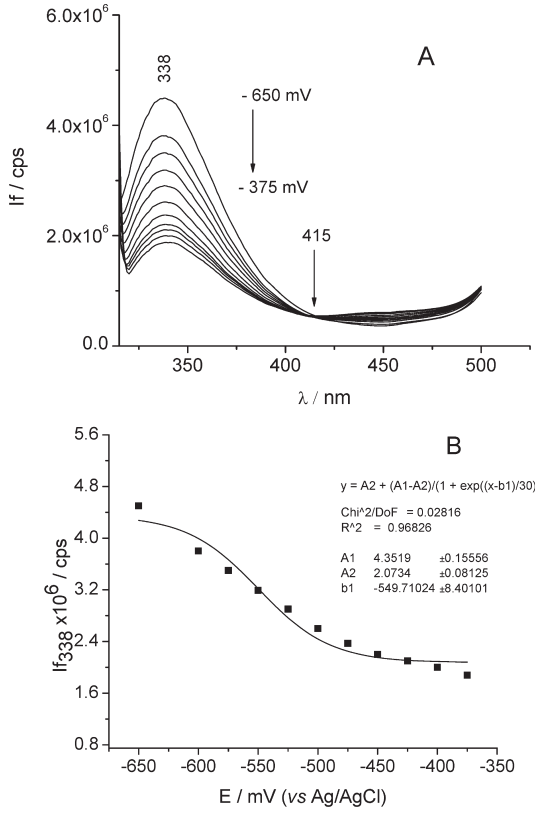

FIGURE 8: Steady-state front-face fluorescence emission spectra (A) and potentiometric titration (B) of SoxS from *P. pantotropus*. The Nernst fit of the fluorescence intensity at 338 nm gave a midpoint potential of −550 ± 8 mV vs Ag/AgCl. The protein concentration was 1.63 mM in 45 mM Tris-HCl (pH 7.4), and the measurements were taken at 5 °C. The excitation wavelength was 295 nm. A potential from −650 to −375 mV was applied.

We note that only small variations between the lowest and highest fluorescence intensities were found. This may be overcome by using a cyanine dye as an external fluorescence probe, which would at the same time be the fluorescent donor. It is known that this kind of cyanine fluorescence probe is able to donate electrons to acceptors in solution with varying efficiency depending on the electron acceptor (*38*). In this way, the fluorescence intensity of the attached cyanine fluorescence probe

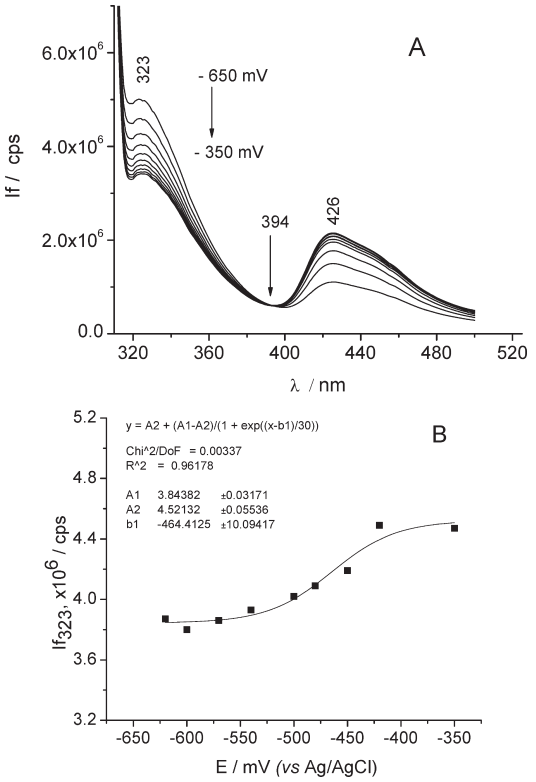

FIGURE 9: Steady-state front-face fluorescence emission spectra (A) and potentiometric titration (B) of SoxW from *P. pantotropus*. The Nernst fit of the fluorescence intensity at 323 nm gave a midpoint potential of −464 ± 10 mV vs Ag/AgCl. The protein concentration was 1.50 mM in 45 mM Tris-HCl (pH 7.4), and the measurements were taken at 5 °C. The excitation wavelength was 295 nm. A potential from −650 to −350 mV was applied.

permits us to distinguish reliably between the oxidized and reduced states of the protein and subsequently measure more accurately the midpoint potential of proteins. The fluorescence detection of a protein's redox state based on resonance energy transfer has been conducted with a fluorescent probe attached to the prosthetic group of the redox protein (*39*).

(*ii*) *Fluorescence Determination of the SoxS and SoxW Protein Redox States*. The coupling of a spectroscopic technique with potentiometric redox titrations is a tool that allows us to determine the redox potential of electron transfer proteins with optically active redox chromophores (*40*).

The redox-dependent steady-state front-face fluorescence emission spectra of the SoxS protein at 338 nm (Figure 8A) could be attributed to the fluorescence of a Trp residue. The data showed that the fluorescence intensity decreased as the potential was changed from −650 to −375 mV. An isosbestic point was found at 415 nm. The potentiometric titration of the SoxS protein is shown in Figure 8B. The Nernst fit of this fluorescence titration revealed a midpoint potential of −550 ± 8 mV versus Ag/AgCl. The fit of the experimental results, lower regression coefficient, R^2 value is 0.97 (add 208 mV for SHE′).

The redox-dependent steady-state front-face fluorescence emission spectra were recorded for SoxW (Figure 9A). Two emission bands could be evidenced. At 323 nm, the emission of a buried Trp decreased with the potential step from −650 to −350 mV. The second emission band at 426 nm increased with potential. This signal may be attributed to the charge transfer emission from Tyr to Trp. An isosbestic point was seen at 394 nm. The potentiometric titration (oxidized minus reduced) of SoxW is

shown in Figure 9B. The Nernst fit of fluorescence titration gave a midpoint potential of −464 ± 10 mV versus Ag/AgCl.

The SoxW protein is redox active in a reversible manner (data not shown), with a slight sigmoidicity of the titration curve. A discrepancy of ∼90 ± 10 mV versus Ag/AgCl between the reductive and oxidative titration was observed. This may be based on the relatively small variation between the lowest and highest fluorescence intensity. Alternatively, a slow equilibration of the protein electrode after the applied reductive potential may explain some of the hysteresis.

CONCLUSION

The combination of front-face fluorescence spectroscopy with the electrochemical technique is of a great interest for the detection of a protein redox state based on the Trp fluorescence emission. It is possible to distinguish between the fully oxidized and fully reduced state of a protein. In this study, the midpoint redox potentials of the SoxS and SoxW proteins were determined by coupling FFFS with an OTTLE cell. According to the potentiometric redox titration, one redox center is available for each of the SoxS and SoxW thioredoxins. The midpoint redox potential for the redox center was −342 ± 8 mV versus SHE for SoxS and −256 ± 10 mV versus SHE for SoxW.

Clear differences were found for the fluorescence spectroscopic properties of both redoxin-like proteins studied here. The differences are based on the Trp in the proximity of the active site, present for SoxS and absent for SoxW. This may be at the origin of the fact that SoxW is not an essential component for inorganic sulfur oxidation of *P. pantotrophus* in vivo.

ACKNOWLEDGMENT

We are indebted to Mr. Xavier Lagrave, Responsible Commercial Fluorescence Molecular and Microanalysis (Horiba Jobin Yvon), for helpful discussions. We thank Martine Heinrich (University of Strasbourg, Strasbourg, France) and Josefina Ringk (Dortmund University of Technology, Dortmund, Germany) for technical assistance and Laurent Fremond for his contributions at the early stage of the project.

REFERENCES

1. Appia-Ayme, C., and Berks, B. C. (2002) SoxV, an ortholog of the CcdA transporter, is involved thiosulfate oxidation in *Rhodovulum sulfidophilum* and reduces the periplasmic thioredoxin SoxW. *Biochem. Biophys. Res. Commun. 296*, 737–741.
2. Friedrich, C. G., Rother, D., Bardischewsky, F., Quentmeier, A., and Fischer, J. (2001) Oxidation of reduced inorganic sulfur compounds by bacteria: Emergence of a common mechanism? *Appl. Environ. Microbiol. 67*, 2873–2882.
3. Friedrich, C. G., Quentmeier, A., Bardischewsky, F., Rother, D., Orawsky, G., Hellwig, P., and Fischer, J. (2008) Redox control of chemotrophic sulfur oxidation of *Paracoccus pantotrophus*. In Microbial sulphur metabolism (Dahl, C., and Friedrich, C. G., Eds.) Chapter 12, pp 139−150, Springer, Berlin.
4. Carius, Y., Rother, D., Friedrich, C. G., and Scheidig, A. J. (2009) The structure of the periplasmic thiol-disulfide oxidoreductase SoxS from *Paracoccus pantotrophus* indicates a triple Trx/Grx/DsbC functionality in chemotrophic sulfur oxidation. *Acta Crystallogr. D65*, 229–240.
5. Rother, D., Ringk, J., and Friedrich, C. G. (2008) Sulfur oxidation of *Paracoccus pantotrophus*: The sulfur-binding protein SoxYZ is the target of the periplasmic thiol-disulfide oxidoreductase SoxS. *Microbiology 154*, 1980–1988.
6. Leger, C., Lederer, F., Guigliarelli, B., and Bertrand, P. (2006) Electron flow in multicenter enzymes: Theory, applications, and consequences on the natural design of redox chains. *J. Am. Chem. Soc. 128*, 180–187.
7. Armstrong, F. A., Butt, J. N., and Sucheta, A. (1993) Voltammetric studies of redox-active centers in metalloproteins adsorbed on electrodes. *Methods Enzymol. 227*, 479–500.
8. Frew, J. E., and Hill, H. A. (1988) Direct and indirect electron transfer between electrodes and redox proteins. *Eur. J. Biochem. 172*, 261–269.
9. Eftink, M. R. (1991) in Methods of Biochemical Analysis (Suelter, C. H., Ed.) pp 127−205, John Wiley, New York.
10. Lakowicz, J. R. (1999) in Principles of Fluorescence Spectroscopy, Kluwer- Plenum, New York.
11. Ruan, K., Li, J., Liang, R., Xu, C., Yu, Y., Lange, R., and Balny, C. (2002) A rare protein fluorescence behavior where the emission is dominated by tyrosine: Case of the 33-kDa protein from spinach photosystem II. *Biochem. Biophys. Res. Commun. 293*, 593–597.
12. Reshetnyak, Y. K., and Burstein, E. A. (2001) Decomposition of protein tryptophan fluorescence spectra into log-normal components. II. The statistical proof of discreteness of tryptophan classes in proteins. *Biophys. J. 81* (3), 1710–1734.
13. Reshetnyak, Y. K., Koshevnik, Y., and Burstein, E. A. (2001) Decomposition of protein tryptophan fluorescence spectra into log-normal components. III. Correlation between fluorescence and microenvironment parameters of individual tryptophan residues. *Biophys. J. 81* (3), 1735–1758.
14. Genot, C., Tonetti, F., Montenay-Garestier, T., Marion, D., and Drapon, R. (1992) Front-face fluorescence applied to structural studies of proteins and lipid-protein interactions of visco-elastic food products. 2. Application of wheat gluten. *Sci. Aliments 12*, 687–704.
15. Parker, C. A. (1969) Apparatus and experimental methods. In Photoluminescence of solutions with applications to photochemistry and analytical chemistry (Parker, C. A., Ed.) pp 128−302, Elsevier, Amsterdam.
16. Herbert, S., Riaublanc, A., Bouchet, B., Gallant, D. J., and Dufour, E. (1999) Fluorescence spectroscopy investigation of acid- and rennet-induced coagulation of milk. *J. Dairy Sci. 82*, 2056–2062.
17. Kakiuchi, T., and Takasu, Y. (1994) Differential cyclic voltfluorometry and chronofluorometry of the transfer of fluorescent ions across the 1,2-dichloroethane-water interface. *Anal. Chem. 66*, 1853–1859.
18. Nagatani, H., Igleasias, R. A., Fermin, D. J., Brevet, P. F., and Girault, H. H. (2000) Adsorption behavior of charged zinc porphyrins at the water/1,2-dichloroethane interface studied by potential modulated fluorescence spectroscopy. *J. Phys. Chem. B 104*, 6869–6876.
19. Jennings, P., Jones, A. C., and Mount, A. R. (2000) *In situ* spectroelectrochemical studies of the fluorescence of 5-substituted indole trimer films. *Phys. Chem. Chem. Phys. 2*, 1241–1248.
20. Stoodley, R., and Bizzotto, D. (2003) Epi-fluorescence microscopic characterization of potential-induced changes in a DOPC monolayer on a Hg drop. *Analyst 128*, 552–561.
21. Taniguchi, I., Fujiwara, T., and Tominaga, M. (1992) New simple cell for in-situ fluoroelectrochemical measurements. *Chem. Lett. 12*, 1217–1220.
22. Farren, C., Christensen, C. A., FitzGerald, S., Bryce, M. R., and Beeby, A. (2002) Synthesis of novel phthalocyanine-tetrathiafulvalene hybrids; intramolecular fluorescence quenching related to molecular geometry. *J. Org. Chem. 67*, 9130–9139.
23. Hu, X., Wang, Q., He, P., and Fang, Y. (2002) Spectroelectrochemistry study on the electrochemical reduction of ethidium bromide. *Anal. Sci. 18*, 645–650.
24. Dias, M., Hudhomme, P., Levillain, E., Perrin, L., Sahin, Y., Sauvage, F.-X., and Wartelle, C. (2004) Electrochemistry coupled to fluorescence spectroscopy: A new versatile approach. *Electrochem. Commun. 6*, 325–330.
25. Chen, Y.-M., and Guo, L.-H. (2009) Combined fluorescence and electrochemical investigation on the binding interaction between organic acid and human serum albumin. *J. Environ. Sci. 21*, 373–379.
26. Chou, J., Qu, X., Lu, T., Dong, S., and Wu, Y. (1995) The effect of solution pH on synchronous fluorescence spectra of cytochrome *c* solutions. *Microchem. J. 52*, 159–165.
27. Farinha, J. P. S., Martinho, J. M. G., and Pogliani, L. (1997) Nonlinear least-squares and chemical kinetics. An improved method to analyse monomer-excimer decay data. *J. Math. Chem. 21*, 131–139.
28. Moss, D., Nabedryk, E., Breton, J., and Mantele, W. (1990) Redox-linked conformational changes in proteins detected by a combination of infrared spectroscopy and protein electrochemistry. Evaluation of the technique with cytochrome *c*. *Eur. J. Biochem. 187*, 565–572.
29. Hellwig, P., Behr, J., Ostermeier, C., Richter, O. M. H., Pfitzner, U., Odenwald, A., Ludwig, B., Michel, H., and Mantale, W. (1998) Involvement of Glutamic Acid 278 in the Redox Reaction of the Cytochrome *c* Oxidase from *Paracoccus denitrificans* Investigated by FTIR Spectroscopy. *Biochemistry 37*, 7390–7399.
30. Aylmer-Kelly, A. W. B., Bewick, A., Cantrill, P. R., and Tuxford, A. M. (1973) Studies of electrochemically generated reaction intermediates

using modulated specular reflectance spectroscopy. *Faraday Discuss. Chem. Soc. 56*, 96–107.
31. Katti, S. K., LeMaster, D. M., and Eklund, H. (1990) Crystal structure of thioredoxin from *Escherichia coli* at 1.68-Å resolution. *J. Mol. Biol. 212*, 167–184.
32. Saarinen, M., Gleason, F. K., and Eklund, H. (1995) Crystal structure of thioredoxin-2 from *Anabaena*. *Structure 3*, 1097–1108.
33. Beechem, J., and Brand, L. (1985) Time resolved fluorescence decay in proteins. *Annu. Rev. Biochem. 54*, 43–71.
34. Alcala, J. R., Gratton, E., and Prendergast, F. G. (1987) Fluorescence lifetime distributions in proteins. *Biophys. J. 51*, 597–604.
35. Orawski, G., Bardischewsky, F., Quentmeier, A., Rother, D., and Friedrich, C. G. (2007) The periplasmic thioredoxin SoxS plays a key role in activation in vivo of chemotrophic sulfur oxidation of *Paracoccus pantotrophus*. *Microbiology 153*, 1081–1086.
36. Moore, G. R., Huang, Z., Eley, C. G., Bark, H. A., Williams, G., Robinson, M. N., and Williams, R. J. P. (1982) Electron transfer in biology: The function of cytochrome *c*. *Farady Discuss. Chem. Soc. 74*, 311–329.
37. Margoliash, E., and Schejter, A. (1995) How does a small protein become so popular? In Cytochrome c: A multidisciplinary approach (Scott, R. A., and Mauk, A. G., Eds.) pp 3−32, University Science Books, Sausalito, CA.
38. Doizi, D., and Mialocq, J. C. (1987) Photosensitized electron-transfer reaction in the first excited singlet-state of a polymethine cyanine dye. *J. Phys. Chem. 91*, 3524–3530.
39. Kuznetsova, S., Zauner, G., Schmauder, R., Mayboroda, O. A., Deelder, A. M., Aartsma, T. J., and Canters, G. W. (2006) A Forster-resonance-energy transfer-based method for fluorescence detection of the protein redox state. *Anal. Biochem. 350*, 52–60.
40. Berczi, A., Caubergs, R. J., and Asard, H. (2003) Partial purification and characterization of an ascorbate-reducible *b*-type cytochrome from the plasma membrane of *Arabidopsis thaliana* leaves. *Protoplasma 221*, 47–56.